

DYNAMIC EDGE TRACING FOR 2D IMAGE SEGMENTATION

D.J. Withey¹, Z.J. Koles¹, W. Pedrycz²

¹Department of Biomedical Engineering, University of Alberta, Canada

²Department of Electrical and Computer Engineering, University of Alberta

Abstract - A novel segmentation technique which may be useful for two dimensional (2D) magnetic resonance (MR) image segmentation is presented. The technique utilizes a dynamic target tracking algorithm and a Kalman filter and permits edges to be followed in the presence of intensity variation similar to that found in MR images. Segmentation of two synthetic test images, one with intensity nonuniformity and one without, is performed. Fuzzy c-means clustering with pixel intensity features is used to segment the same test images for qualitative comparison.

Keywords - Image segmentation, edge tracing, Kalman filter, intensity nonuniformity.

I. INTRODUCTION

Magnetic Resonance (MR) images are excellent sources of patient-specific anatomical information. Automatic segmentation of these images into component tissue classes provides a method for reproducible extraction of this information. One problem that complicates this process, however, is intensity nonuniformity, an artifact in MR images which is evident as a gradual variation in intensity over otherwise identical tissue classes. Intensity nonuniformity has several causes, notably, inhomogeneity in radio frequency (RF) transmitter and receiver coils during image acquisition [1].

MR images provide excellent soft tissue contrast so that intensity-related features are natural choices for use with automatic segmentation methods. However, compensation for intensity nonuniformity must be included in order for such methods to be effective.

Although it is possible to perform some compensation during image acquisition, equipment or protocol modifications are typically required. Furthermore, retrospective application of these corrective measures is not possible. Therefore, compensation applied as a post-processing step is considered to be desirable [2].

Adaptive fuzzy c-means [2], [3], and statistically-based methods [4], [5] are examples of techniques which have been developed to perform automatic image segmentation in the presence of MR intensity nonuniformity. Other methods, such as nonlinear filtering [6], are intended to address the nonuniformity independently, permitting subsequent segmentation of the intensity corrected image.

Image segmentation can be performed by voxel labeling, involving classification of each image voxel or by identification of the bounding surfaces of objects in the image. The adaptive fuzzy c-means methods [2], [3] and the statistical methods [4], [5] are examples of techniques which perform voxel labeling.

Determining the object boundaries in two dimensional images can be done by application of active contours [10] or by edge tracing [11]. We describe a technique for edge tracing

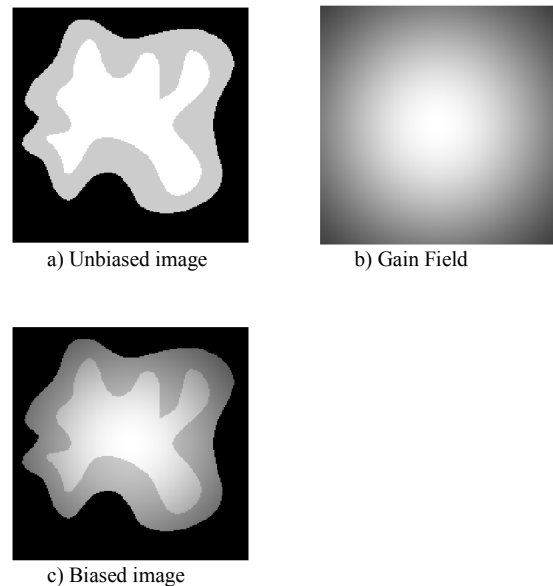


Fig. 1 Synthetic test images.

which includes a Kalman filter and a dynamic target tracking algorithm to associate edge pixels into object boundaries.

II. METHODOLOGY

A. Synthetic Images

Fig. 1 panels (a), and (c) show the two synthetic test images. The shapes of the objects in the images have been chosen to resemble cortical gray matter and white matter in MR images of the brain. Each image has size of 200x200 pixels with 256 gray levels. The unbiased image was formed by interpolating a small set of points with cubic splines to form boundaries of closed regions. These boundaries were then converted to discrete pixels and the enclosed regions were filled with a selected gray level value. The unbiased test image has three gray levels with a difference of fifty gray levels between the brightest region and the intermediate intensity level.

In MR images, intensity nonuniformity has been approximated by exponential functions [1]. For the test images, the gain field (g), which simulates the intensity nonuniformity, was formed using a two dimensional exponential function:

$$g = \exp(-k_1(X - X_c)^2 - k_2(Y - Y_c)^2) \quad (1)$$

where (X, Y) are pixel coordinates and (X_c, Y_c) are the coordinates of the image centre. Parameters k_1 and k_2 were

Report Documentation Page

Report Date 25 Oct 2001	Report Type N/A	Dates Covered (from... to) -
Title and Subtitle Dynamic Edge Tracing for 2D Image Segmentation	Contract Number	
	Grant Number	
	Program Element Number	
Author(s)	Project Number	
	Task Number	
	Work Unit Number	
Performing Organization Name(s) and Address(es) Department of Biomedical Engineering University of Alberta Canada	Performing Organization Report Number	
Sponsoring/Monitoring Agency Name(s) and Address(es) US Army Research, Development & Standardization Group (UK) PSC 802 Box 15 FPO AE 09499-1500	Sponsor/Monitor's Acronym(s)	
	Sponsor/Monitor's Report Number(s)	
Distribution/Availability Statement Approved for public release, distribution unlimited		
Supplementary Notes Papers from 23rd Annual International Conference of the IEEE Engineering in Medicine and Biology Society, October 25-28, 2001, held in Istanbul, Turkey. See also ADM001351 for entire conference on cd-rom.		
Abstract		
Subject Terms		
Report Classification unclassified	Classification of this page unclassified	
Classification of Abstract unclassified	Limitation of Abstract UU	
Number of Pages 4		

chosen to provide a fifty percent intensity reduction at the image edges along the principal axes.

The biased image was formed by multiplying the unbiased image by the gain field, thus simulating an image with intensity nonuniformity.

B. Fuzzy c-Means Clustering

Fuzzy c-means clustering is a pattern recognition technique which is used in image segmentation [7]. Each pixel is evaluated according to a selected feature set, forming a set of vectors, or a set of points, in the feature space. Clusters are regions in the feature space with a high density of such points. A prototype vector, or cluster centre for each cluster is found by an iterative computation that minimizes the objective function

$$F = \sum_{k=1}^N \sum_{i=1}^c u_{ik}^m \times D_{ik}^2 \quad (2)$$

where c is the number of clusters to form, N is the number of pixels in the image, m is the fuzzification factor (typically chosen to be 2), u_{ik} is the membership of pixel k in cluster i , $D_{ik} = \|f_k - v_i\|$ is the distance between the k th feature vector (f_k) and the i th prototype vector (v_i). Once the prototype vectors and membership values have been found, each pixel can be assigned to the class of maximum membership to complete the segmentation.

Fuzzy c-means clustering is used here to demonstrate the problem that can occur when image segmentation is performed without attention to the effect of nonuniform intensity. The features selected for each pixel are the pixel intensity and the intensity of the four nearest neighbours. The number of clusters is three (ie. $c = 3$) and the fuzzification factor is 2.

C. Dynamic Edge Tracing

Segmentation by edge tracing involves edge detection followed by association of edge pixels into object boundaries. In the case of the edge tracing method described here, edge detection is performed on the input image followed by a line by

line scan of the edge image. On each line scan, the edge pixel positions and image intensity at the edge pixel are used as input to a multiple target, dynamic tracking algorithm. The scanning procedure introduces a history, allowing edges in the image to be followed along what amounts to a time dimension. Each new line brings a set of updated edge positions which are then associated with existing edge data from the previous lines. Edge positions that cannot be associated with an existing track are used to start two new tracks, one to the left and one to the right of the scan direction. Tracks which follow the same edge but in different directions will terminate on each other. These occurrences and the common start points are used to assemble the edges at the end of the scan.

The effective “movement” of the edge from one line to the next during the image scan simulates a dynamic system. Dynamic systems, linear or nonlinear, are described by state and state transitions. State is a quantitative description of past and present behaviour, sufficient information to predict future behaviour. State transition is the description of how one state is transformed into another. For example, in aircraft tracking, state would include the position and velocity of the aircraft. The aircraft position could be predicted at a future time based on its current position and current velocity.

Automatic tracking algorithms are normally used to monitor the movement of aircraft or other targets of interest [8]. In the classical target tracking application, sensors provide measurements of the target state (eg. position and velocity) to the tracking system at equal time intervals. The measured target data is compared to predicted target data and if sufficient correlation exists, the measured data is incorporated into the target history and a new prediction is formed for the next input sample. In this way, observations taken at different times can be associated together and the path taken by the target can be followed.

The functions of the tracking system are data association and state estimation. Data association is the process by which new data is correlated with existing data and the path of a target is updated. State estimation is the process whereby a target state estimate is computed using *a priori* noise statistics and past samples and whereby a predicted target state is determined. The target state estimate and next sample prediction are produced by a tracking filter with the prediction presented to the data association process at the next time interval. A block diagram of such a tracking system is shown in Fig. 2.

In the edge tracing method described here, the tracking filter used for state estimation is a Kalman filter [9], the recursive solution to the discrete time, linear, minimum variance estimation problem and the statistical estimator most often used in dynamic tracking [8]. For a given track, the Kalman filter is used to predict the edge position on the next line, facilitating the association of the next set of edge positions into the existing edge tracks.

The Kalman filter is defined with the assumptions of a linear, dynamic system and zero mean, gaussian noise. Gaussian distributions and linear dynamics are natural assumptions especially if statistical data is not largely available [9].

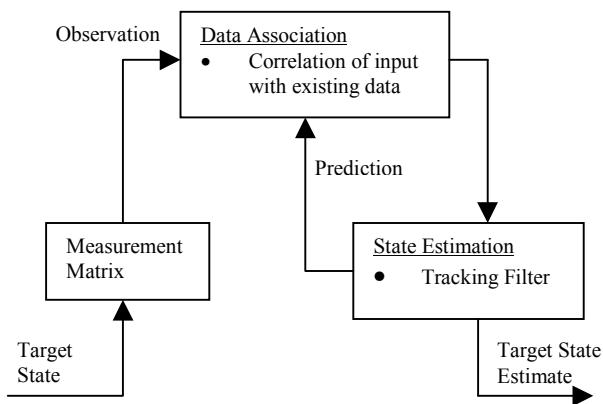


Fig. 2. Tracking System Block Diagram

The Kalman filter can be used to estimate the state of a discrete process that is governed by the linear, stochastic difference equation

$$x_{k+1} = A_k x_k + w_k \quad (3)$$

where k is the step counter, x_k is the state vector at step k , A_k is the state transition matrix, and w_k is the process noise vector. The process noise is assumed to be zero mean with gaussian statistics. Measurements related to the target are also assumed to contain zero mean, gaussian noise:

$$z_k = H_k x_k + v_k \quad (4)$$

where z_k is the measurement vector at step k , H_k is the measurement matrix, and v_k is the measurement noise vector.

The actual state of the target is not known and the Kalman filter is used to estimate it from the measurement and a previously determined state prediction. The estimate is taken to be a linear combination of the prediction and the difference between the measurement and the predicted measurement.

$$\hat{x}_k = \hat{x}_k^- + K_k (z_k - H_k \hat{x}_k^-) \quad (5)$$

where \hat{x}_k is the state estimate at step k , \hat{x}_k^- is the state prediction at step k , and K_k is the Kalman filter gain. Also, the error covariance matrices are given by:

$$P_k = E\{(x_k - \hat{x}_k)(x_k - \hat{x}_k)^T\} \quad (6)$$

$$P_k^- = E\{(x_k - \hat{x}_k^-)(x_k - \hat{x}_k^-)^T\} \quad (7)$$

where P_k is the *a posteriori* error covariance matrix, P_k^- is the *a priori* error covariance matrix, and $E\{\}$ represents mathematical expectation. The Kalman filter gain (K_k) is determined by minimization of the error covariance matrix (P_k) [9], [12].

At each measurement interval the Kalman filter gain matrix, state estimate vector, and error covariance matrix are updated.

$$K_k = P_k^- H_k^T (H_k P_k^- H_k^T + R_k)^{-1} \quad (8)$$

$$\hat{x}_k = \hat{x}_k^- + K_k (z_k - H_k \hat{x}_k^-) \quad (9)$$

$$P_k = (I - K_k H_k) P_k^- \quad (10)$$

where $R_k = E\{v_k v_k^T\}$ is the measurement noise covariance matrix and I is the identity matrix.

Prediction of the next state is also done at each time interval

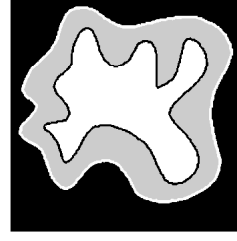
$$\hat{x}_{k+1}^- = A_k \hat{x}_k \quad (11)$$

$$P_{k+1}^- = A_k P_k A_k^T + Q_k \quad (12)$$

where $Q_k = E\{w_k w_k^T\}$ is the process noise covariance matrix.

The data association process will utilize the predicted error covariance matrix to form a bounding window around the predicted measurement. Any measurement that appears within this window is a candidate for association.

We use a simple two state filter where target state consists of position and velocity and the measurement is of position



a) Edge tracing
- unbiased image.



b) Fuzzy clustering
- unbiased image.



c) Edge tracing
- biased image.



d) Fuzzy clustering
- biased image.

Fig. 3. Segmentation results.

only. Under these conditions, A_k and H_k can easily be defined. That is, for

$$x_k = [X, Y, \dot{X}, \dot{Y}]^T \quad (13)$$

where (X, Y) represents the target position in two dimensions and (\dot{X}, \dot{Y}) represents the target velocity in two dimensions and assuming a unit time step, the state transition and measurement matrices become:

$$A_k = \begin{bmatrix} 1 & 0 & 1 & 0 \\ 0 & 1 & 0 & 1 \\ 0 & 0 & 1 & 0 \\ 0 & 0 & 0 & 1 \end{bmatrix} \quad (14), \quad H_k = \begin{bmatrix} 1 & 0 & 0 & 0 \\ 0 & 1 & 0 & 0 \end{bmatrix} \quad (15)$$

which is to say that the next target state will be estimated from the current position and current velocity, that only position is measured, and that no particular measurement correction is required. Furthermore, these two matrices will remain constant for all k .

Our calculations are done in this manner with the exception that three dimensions are used, these being the two coordinates of the edge pixel and the image intensity at the edge pixel location.

III. RESULTS

Fig. 3 shows the results from segmentation of the unbiased and biased test images by the edge tracing technique and by the fuzzy clustering approach. Panels (b) and (d) show that clustering works well when the intensity is uniform (b) but that

given sufficient intensity nonuniformity, errors occur in the pixel assignments. In Panel (d), peripheral portions of the high intensity region are classed with lower intensity pixels and the central portion of the high intensity region is expanded, exhibiting a circularly shaped artifact due to the exponentially shaped intensity variation.

The results from the dynamic edge tracing algorithm are shown in (a) and (c). In each case, the high intensity region is outlined with a black contour and the medium intensity region is outlined with a white contour. These lines coincide with the edge pixels very well.

The fit was evaluated by reconstructing the test image using each of the two sets of edge contours. Upon comparison with the original, unbiased test image, it was found that the reconstruction using contours from the unbiased image segmentation contained one pixel classified incorrectly. The reconstruction using contours from the biased image segmentation contained ten misclassified pixels, amounting to 0.025 percent of all image pixels.

IV. DISCUSSION

Quantitative comparison of the fuzzy clustering result with the edge tracing result is not intended, however, having the two side by side gives an opportunity to examine the advantages of each. Although fuzzy clustering requires that the number of classes be known *a priori*, it can be extended to perform segmentation of three dimensional (3D) images relatively easily. The edge tracing method does not require the number of tissue classes to be known *a priori* but is not as easily extended to 3D.

When 2D images are considered, operation without *a priori* knowledge of the number of tissue classes is a big advantage especially if the goal is automatic analysis of images where pathology may be involved. Fuzzy clustering may not position a cluster prototype so as to identify a relatively small region of distinct intensity in an image when there are much larger numbers of pixels in other intensity groups. Consideration of the objective function in (2) will confirm this. Since the objective function is based on minimizing the sum of all distances, a small but distinct group in the feature space may not have enough accumulated distance to attract a cluster centre. The edge tracing technique, however, would find all regions where there is an identifiable edge.

Edge tracing methods require some degree of edge continuity to be successful [11]. The edge tracing technique described here does not require adjacent pixel connectivity. Since the edge position is permitted to have a "velocity", the current velocity for that edge will determine where the algorithm searches for the next edge pixel.

V. CONCLUSION

Edge detection followed by a line by line scan of the edge image simulates a dynamic system where the edge position "moves" as the scan proceeds. The application of a dynamic tracking algorithm allows the edge to be followed, permitting edge pixels to be associated into object boundaries. Edge

tracing performed in this manner and using three dimensions (the two edge pixel position coordinates and the image intensity at the edge pixel position) appears to be a viable method for 2D image segmentation in the presence of image intensity nonuniformity.

REFERENCES

- [1] B.R. Condon, J. Patterson, D. Wyper, A. Jenkins, D.M. Hadley, "Image non-uniformity in magnetic resonance imaging: its magnitude and methods for its correction," *Br. J. Radiol.* vol. 60, pp. 83-87, January 1987.
- [2] S.K. Lee, M.W. Vannier, "Post-acquisition correction of MR inhomogeneities," *Magn Reson Med*, vol. 36, pp. 275-286, 1996.
- [3] D.L. Pham, J.L. Prince, "Adaptive fuzzy segmentation of magnetic resonance images," *IEEE Trans. Med. Imag.* Vol. 18, no. 9, pp. 737-752, September, 1999.
- [4] K. Held, E. Rota Kops, B.J. Krause, W.M. Wells III, R. Kikinis, H.-W. Muller-Gartner, "Markov Random Field Segmentation of Brain MR Images," *IEEE Trans. Med. Imag.* Vol. 16, no. 6, pp. 878-886, December, 1997.
- [5] K. Van Leemput, F. Maes, D. Vandermeulen, P. Suetens, "Automated model-based bias field correction of MR images of the brain," *IEEE Trans. Med. Imag.* Vol. 18, no. 10, pp. 885-896, October, 1999.
- [6] B.H. Brinkmann, A. Manduca, R.A. Robb, "Optimized homomorphic unsharp masking for MR grayscale inhomogeneity correction," *IEEE Trans. Med. Imag.* Vol. 17, no. 2, pp. 161-171, April, 1998.
- [7] J.C. Bezdek, L.O. Hall, L.P. Clarke, "Review of MR image segmentation techniques using pattern recognition," *Med. Phys.* Vol. 20, no. 4, Jul/Aug 1993, pp. 1033-1048.
- [8] E. Waltz, J. Llinas, *Multisensor Data Fusion*. Artech House, 1990.
- [9] R.E. Kalman, "A New Approach to Linear Filtering and Prediction Problems," *Transactions of the ASME - Journal of Basic Engineering*, March, 1960, pp. 35-45.
- [10] M. Kass, A. Witkin, D. Terzopoulos, "Snakes: Active contour models," *Int. J. Comput. Vision*, vol. 1, 1988, pp. 321-331.
- [11] M. Lineberry, "Image segmentation by edge tracing," in proc. of SPIE, The International Society for Optical Engineering, vol. 359, *Applications of Digital Image Processing 4*, San Diego, Calif., USA, 1982, pp. 361-368.
- [12] G. Welch, G. Bishop, "An Introduction to the Kalman Filter," *Report TR 95-041*, University of North Carolina at Chapel Hill, Nov. 2000.